

# Experimental Tests of Wind Turbine Main Shaft Motion on a Laboratory Test Rig

Dirk Lutschinger<sup>1</sup>, Ian Howard<sup>2</sup>

<sup>1,2</sup>*Curtin University, Perth, Western Australia, 6845, Australia*

*d.lutschinger@curtin.edu.au*

*I.Howard@exchange.curtin.edu.au*

## ABSTRACT

This paper introduces research and discusses findings dealing with failure modes of gearboxes in wind turbines. These gearboxes fail in general after five years which is far below the expected design life of twenty years of a wind turbine. The research is taking a more holistic approach towards finding typical behaviour of the main shaft taking the transient nature of the wind into consideration. In this research, a small scale wind turbine test rig has been designed and manufactured with displacement sensors installed to observe the displacement of the main shaft at specific points, namely the main bearing locations of the forward framework of a wind turbine nacelle, where the main shaft is installed. The experimental data measured from the test rig is being analysed with common beam bending, statistical and fatigue theories to draw conclusions for long term loading in service. Aspects of the turbulent nature of the wind driving the wind turbine have been taken into consideration as being part of the aerodynamic loading onto the rotor and eventually the gearbox, transmitted through the main shaft. The purpose of the test rig at this stage is to obtain a quantitative insight into the motion of the main shaft. The deliberately chosen softer aluminum material and the more slender geometry for the components should provide exaggerated displacements which help to make motion and deformations more obvious. At this point, no resemblance to real size wind turbines has been established.

## 1. INTRODUCTION

Gearboxes of horizontal wind turbines have a tendency to fail in service before the end of the design life of the wind turbine itself (Van Rensselar, 2010). According to Musial, Butterfield and McNiff (2007), the failure of the gearbox begins in the bearings of the gears inside the gearbox. In this project an experimental approach is conducted to determine

the typical motion of the main shaft that connects the rotor hub with the gearbox. The shaft is in general rigidly connected with the carrier arm of the first planetary stage through a ring that applies pressure onto the surfaces of both components (Rexroth Bosch Group, 2010). Figure 1 shows a sketch of a typical gearbox with three planetary stages used in wind turbines. The above mentioned rigid connection is visible here as well. Misalignments between the main shaft and the first planetary stage are expected to contribute to the failure problems. Also indicated are typical gear shaft or carrier arm bearing locations. Moser (2010) states that one reason for the gearbox failure is the turbulent nature of the wind. The flow field around a wind turbine in real wind situations is turbulent. It has randomly distributed eddies with small and large sizes. These eddies hit the three blades of a rotor, a three bladed rotor assumed, with different speeds and under different angles at different locations along the blades. Hence they are expected to cause different local aerodynamic forces which apply a resultant moment onto the hub of the rotor which is changing in magnitude and direction over time.

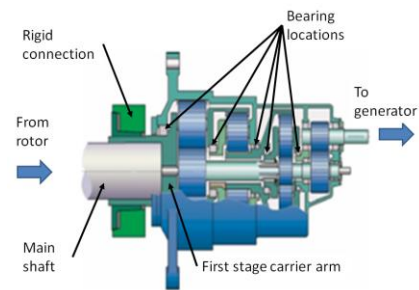


Figure 1. Typical gearbox layout (Rexroth Bosch Group, 2010)

The experimental design in this research has a main shaft realised with two main bearings holding the shaft. The displacements of these bearings in the plane perpendicular to the main shaft have been measured. In particular the displacements along two axes, orthogonal to each other have been recorded over time. The entire experiment has taken place in a test set up in a laboratory. The set up comprised

Dirk Lutschinger et al. This is an open-access article distributed under the terms of the Creative Commons Attribution 3.0 United States License, which permits unrestricted use, distribution, and reproduction in any medium, provided the original author and source are credited.

of three main components, a fan, an aerodynamic element, and a wind turbine test rig. As a fourth component, a board

containing the electrical devices for the measurement equipment has been constructed. Figure 2 illustrates the overall experimental setup of the four components.

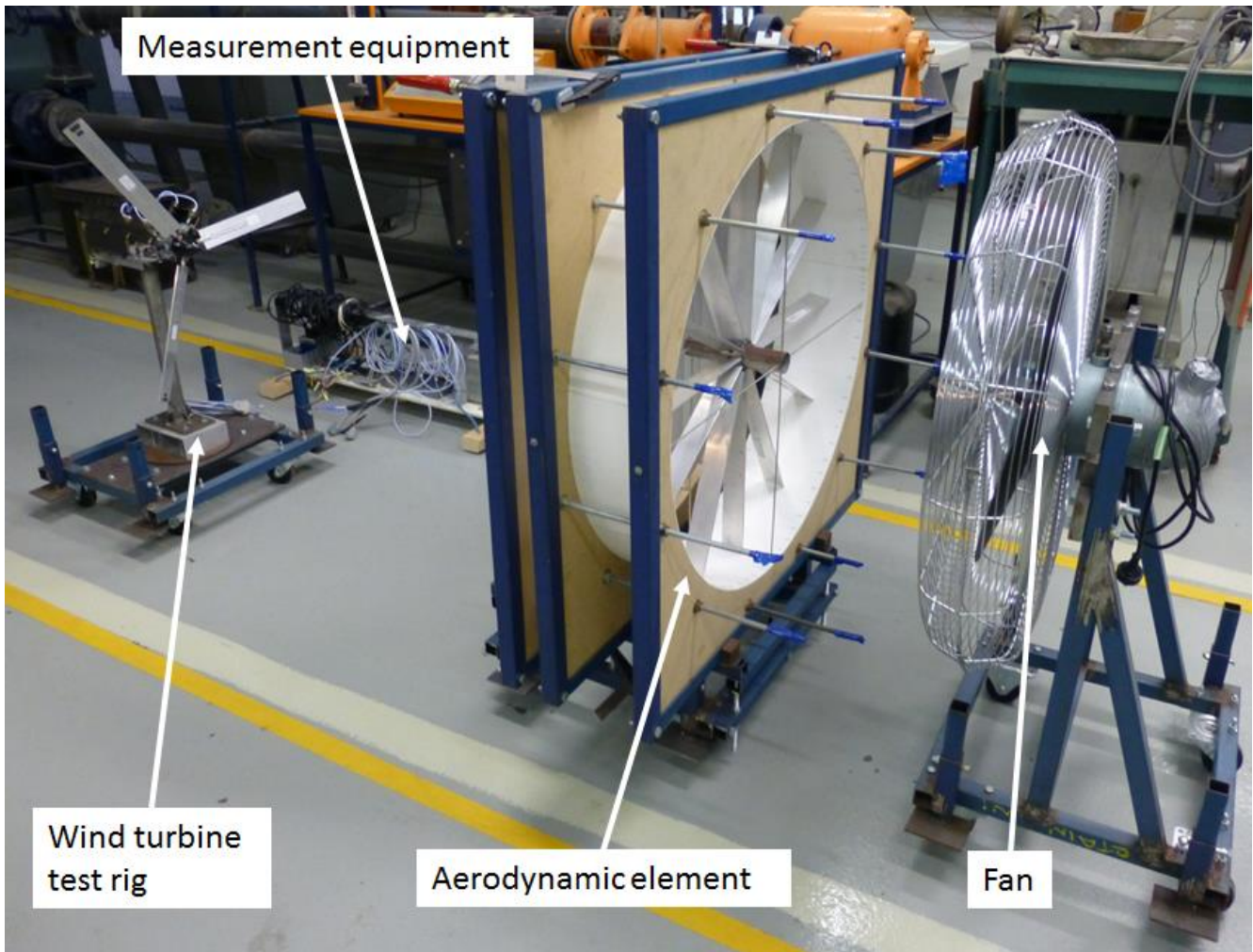


Figure 2. Wind Turbine test set up

## 2. EXPERIMENTAL TESTS

### 2.1. Wind Simulation

The tests were performed inside a laboratory with a conventional industrial fan as the flow source. The flow behind a fan, according to Eck (1973) is built up as a concentrated flow with rotation and a vortex core inside, parallel to the flow direction and centered around the central line of the hub of the fan. To straighten the flow again and to get rid of the vortex, an aerodynamic construction has been installed behind the fan. It consists of a stator and

vertical vanes. This design has been taken over from general arrangements of low-speed wind tunnels as described by Pope & Harper (1966). This component, that is actually acting as sort of an aerodynamic filter can be seen in Figure 2 in the center of the image.



Figure 3: Flow vortex behind fan (left) and straightened flow with aerodynamic element (right)

After placing the “aerodynamic filter” downstream of the fan, a more even flow was obtained. In the left side of Figure 3, the flow with the vortex after the fan, visualized with cotton strips, can be seen whereas on the right side of the figure, the straightened flow has been made obvious with the cotton strips. Test campaigns have been performed to investigate the wind speeds downstream at designated locations. For that a micromanometre has been used. It was connected to a pitot tube that has been placed onto the central line at the height of the hub of the fan. Measurements were taken downstream in 1 meter steps up to 4 meters away from the “aerodynamic filter”. Measured data has been put together in Table 1. The values represent overall wind speeds and their fluctuations in meters per seconds. The first column divides the table into three different fan rotational speed levels with 1 being the slowest and 3 the fastest.

The measurements showed that for distances greater than 3 meters the fluctuation of the speeds significantly increased. This was also experienced with a simple hand test placing the hand into the flow and “feeling” the change of the pressure induced onto the hand’s surface by the flow. Through this test a more turbulent flow in this general area was assumed. The measurements of main shaft displacements were conducted with the wind turbine test rig being positioned 3 metres behind the straightener vanes, in the transient wind speed zone.

## 2.2. Main Shaft Motion

The test rig was designed in a way so that the basic structure of a main shaft and gearbox installation has been realised with two main shaft bearings and the corresponding brackets to hold them as well as the bracket to hold the gearbox. This structure could be seen in Figure 4 in a design example from Rexroth Bosch. The gearbox in the experiment has not been reproduced with gears but only the

front wall and the bearing holding the main shaft in the front wall of the gearbox has been installed. To simulate the total inertia of the gearbox a basic calculation was performed with methods from machine dynamics. As a geometrical reference, the gear arrangement sketched in Figure 1 has been used. A fly wheel with a corresponding inertia has been manufactured and installed onto the shaft. The two main shaft brackets with the main shaft bearings, shown in Figure 5 as Bearing 1 and Bearing 2, have been designed with two blocks each on extensions with a relative angle towards each other of  $90^\circ$  and  $45^\circ$  towards the horizontal. This has the purpose to measure displacements of the blocks with proximity probes. The sizes of the blocks have been chosen according to requirements from the proximity probe handbook to build up the necessary eddy current to function properly. The distance of the blocks from the rotational axis has been chosen for the same reason. There are two proximity probes for each main shaft bearing, measuring the displacements in two axes perpendicular to each other. The probes themselves have been mounted onto steel brackets to keep their movements negligible in relation to the aluminium shaft and bracket arrangement. The shaft continues through the gearbox wall and the bearing where the main shaft enters the gearbox.

Table 1. Flow speeds and fluctuations in [m/s] at different distances behind the straightener vanes for different fan speed settings

Fan level	1 [m]	2 [m]	3 [m]	4 [m]
1	$6.0 \pm 0.3$	$6.2 \pm 0.5$	$5.1 \pm 0.6$	$4.2 \pm 0.7$
2	$6.6 \pm 0.2$	$6.9 \pm 0.4$	$5.4 \pm 0.5$	$4.5 \pm 0.8$
3	$7.0 \pm 0.5$	$7.1 \pm 0.2$	$5.7 \pm 0.4$	$4.9 \pm 1.1$



Figure 4. Main shaft and bearing framework example (Rexroth Bosch Group, 2010)

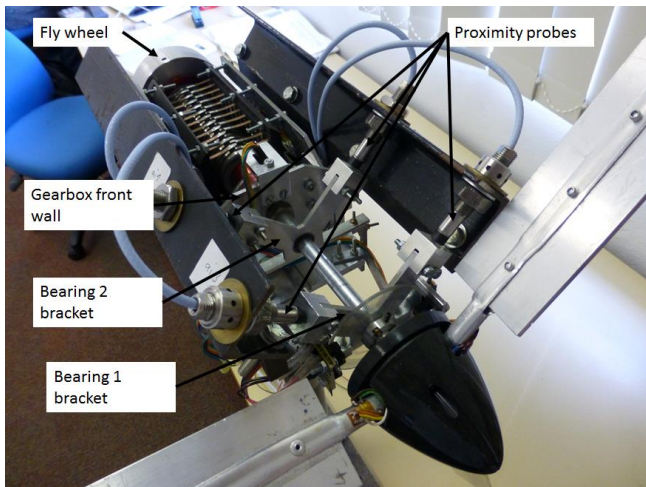


Figure 5. Wind turbine test rig component arrangement

### 3. THEORETICAL CONSIDERATION

#### 3.1. Forces on blades and resulting moment in rotor hub

The theoretical approach taken in this project to deal with the aerodynamic forces on each blade is to assume a resulting aerodynamic force in the so called pressure point of the blade, depending on the flow around it. The flow environment is considered highly turbulent, with eddies of different sizes and flow velocities at different locations in the flow field at one point in time, as can be seen simply sketched in Figure 6. Every blade will experience a different flow and hence a different magnitude and direction of the resulting aerodynamic force and also the pressure point will be at a different location or radius from the rotational axis of the rotor. This resulting force can then be split up into its components in the rotational plane of the rotor and perpendicular to this plane, parallel to the rotational axis, as shown in Figure 7.

Here the pressure point has been labeled as C, the corresponding radii are shown with  $r$  and the two force components, one in-plane, A, and out-of-plane, B, all

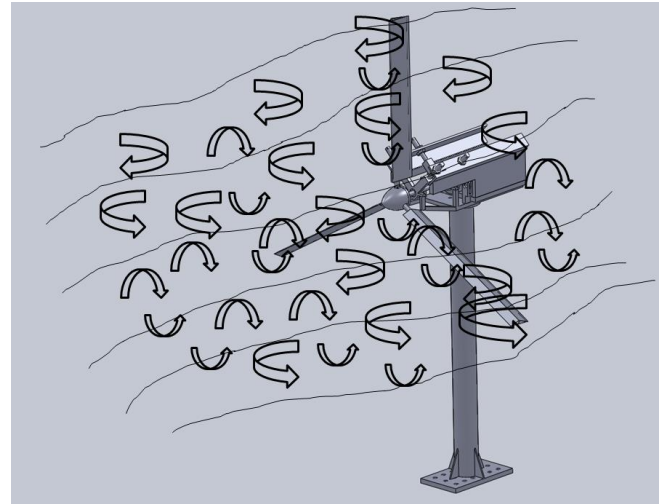


Figure 6. Sketched turbulent wind flow with eddies

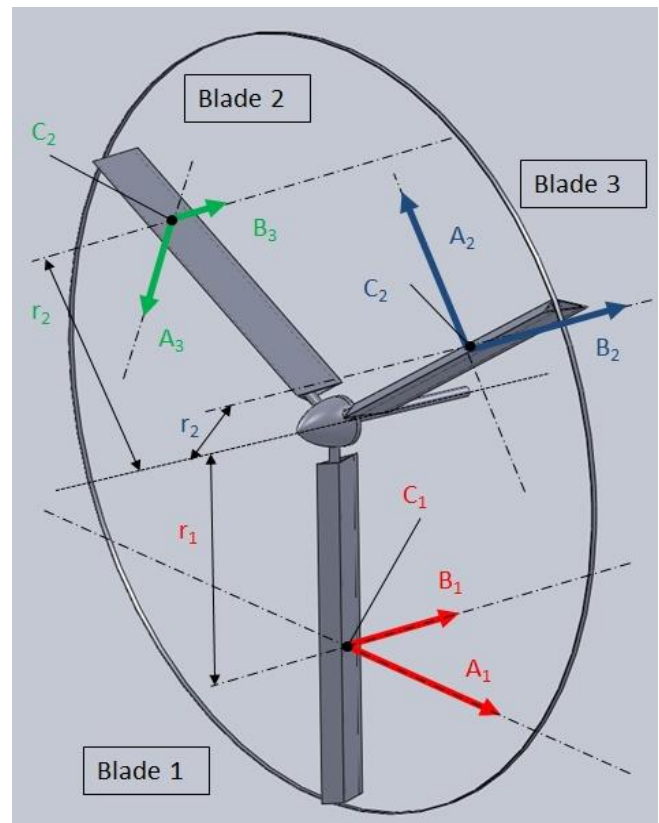


Figure 7. Aerodynamic force components on individual blades

individually numbered for the three blades. When only the B force components are considered, then together with their radii, they create a resulting moment in the rotor hub, in a

plane through the main shaft axis, oriented in space depending on the magnitude of the individual moments of each blade.

Components A contribute to the rotational motion of the rotor. The effect that this moment has on the main shaft is, as expected from simple beam bending theory, a deformation of the framework holding the main shaft. This deformation will be restrained at the bearing locations on the main shaft. However, since the framework has a certain stiffness and is not assumed rigid here, certain displacements of the bearings can be observed. A free body diagram of the main shaft with the external loading moment  $M_a$  and the bearing supports along with their displacements  $\delta_1$  and  $\delta_2$  for the two bearings can be seen in Figure 8.

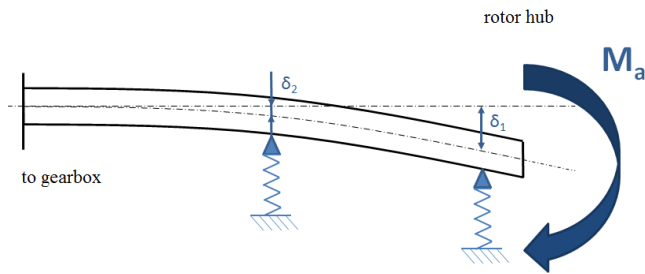


Figure 8. Free body diagram of main shaft

In this figure, the stiffness of the framework and the stiffness of the bearing brackets in particular, have been represented as springs.

#### 4. TEST RESULTS AND ANALYSIS

For a more common method of viewing the main shaft movement, the displacement data can be mathematically transformed into horizontal and vertical components. Figure 9 and Figure 10 represent orbit plots, where the vertical displacement component of a bearing is plotted against its corresponding horizontal displacement component. This is shown in Figure 9 for Bearing 1 and in Figure 10 for Bearing 2. When plotted in this fashion, it is obvious that the shaft is mainly oscillating in the vertical plane through the main shaft central axis. For Bearing 1 the magnitude of the horizontal amplitude around the middle axis is only about 15% of the magnitude of the amplitude in the vertical plane. For Bearing 2, this relation is 11.5%. In the plots, a certain deviation from the vertical plane is visible.

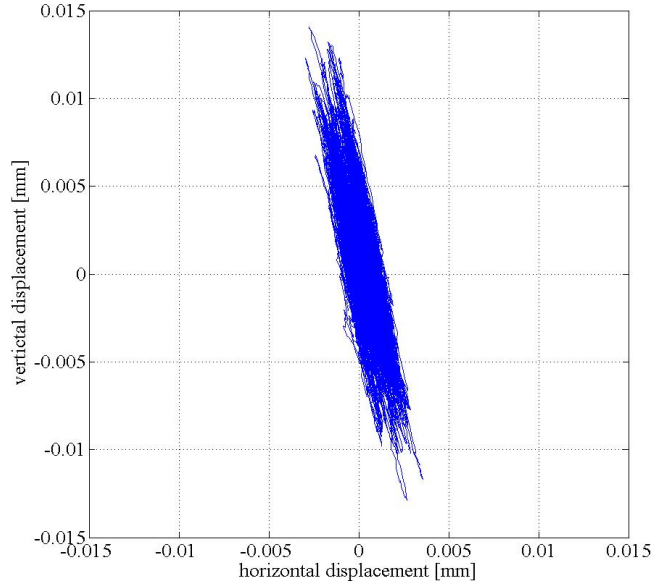


Figure 9. Orbit plot Bearing 1

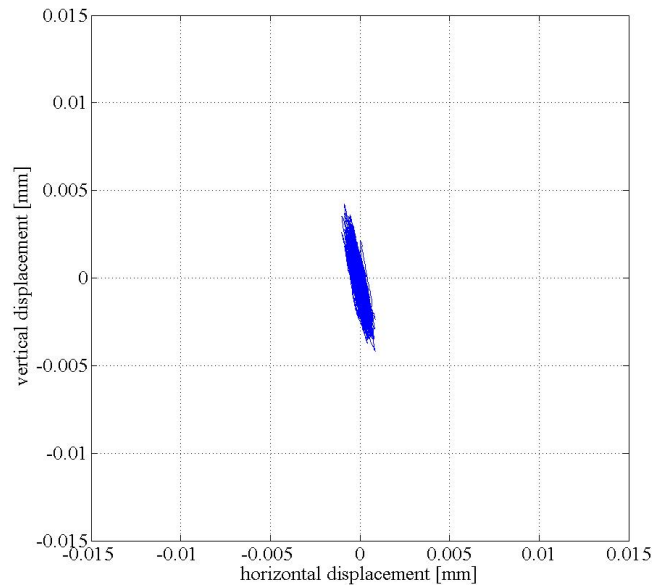


Figure 10. Orbit plot Bearing 2

It has been assumed to be caused by an asymmetrical geometrical error of the test rig construction. Further investigation will be conducted to shed light onto this effect in following tests. Disregarding this effect, it still allows for the simplified approach of assuming the main shaft being alternately bent in more or less a vertical plane. Figure 11 is an extract of the data from this experiment. The curves represent the vertical displacements for Bearing 1 and Bearing 2. It is clearly seen that the direction of displacement for the two bearings relative to each other is

the same. When Bearing 1 is moving upward, Bearing 2 does the same movement and there is no counteracting movement of the two bearings.

Figure 12 shows a close up of the structure that holds the bearings and hence the main shaft. By inspection, and not quantifying any values, the design suggests that the stiffness in the horizontal plane of this framework is much higher than in the vertical plane of the main shaft. It is suspected that this fact contributes to the orbital plots appearing the way they do with a larger amplitude in the vertical plane compared to the horizontal. A moment that is applied at the

hub, resulting from aerodynamic loads, as described in section 3.1, will see its vertical component having a higher bending effect onto the main shaft than its horizontal component. Therefore, in further investigations in this paper, for simplifying reasons, only the vertical displacements are being considered.

Two different effects can be considered for the displacements of the main shaft, when it is continued through the gearbox wall.

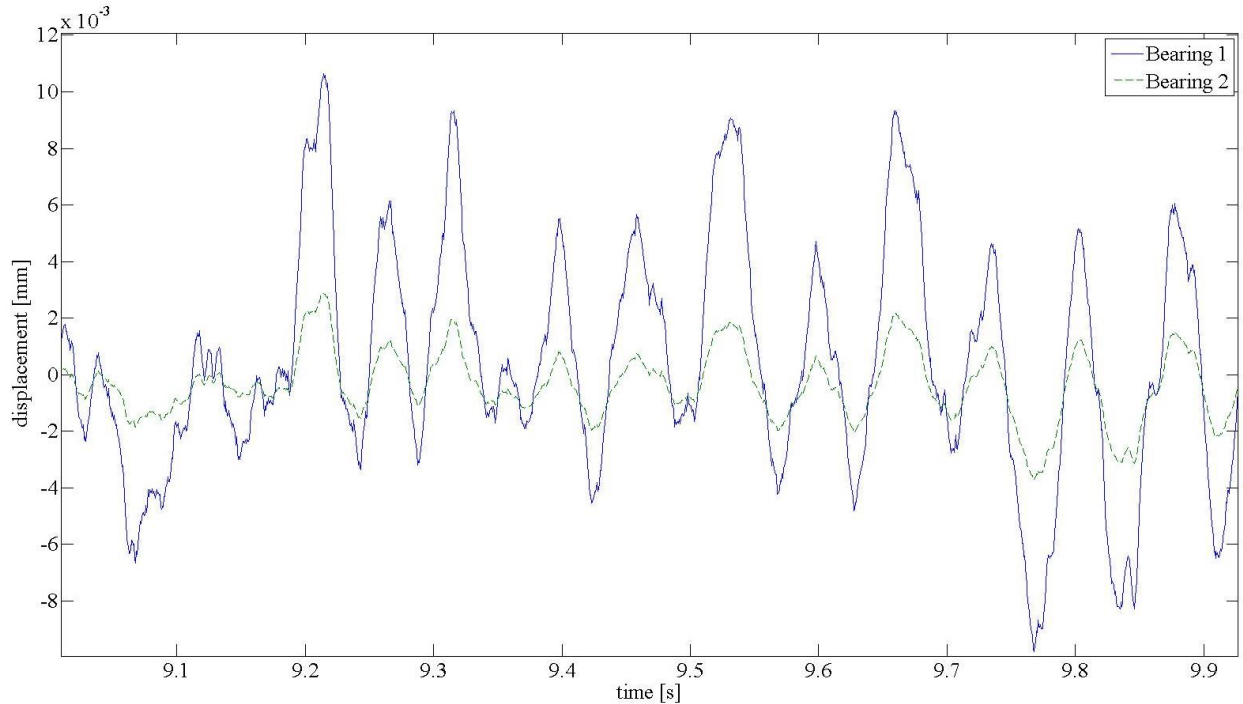


Figure 11. Vertical displacements Bearing 1 and Bearing 2

Firstly, if the first bearing in the gearbox can be considered to have a certain angular clearance when a moment is applied, there will be limited resistance from the bearing against the bending moment. The resulting angular displacement, which in beam bending theory is the slope of the bending curve, will be transmitted into the first gear stage of the gearbox. An oscillating movement of the kind detected in this experiment is likely to cause a damaging effect over a longer period of time in the gearbox.

Secondly, if the bearing does not allow for any movement due to the moment from the main shaft, then the bearing, which is generally made from a harder material than the gearbox wall, would be expected to follow the main shafts angular movement. This will effectively bend and distort the gearbox wall, having a similar effect on the first gear stage. Again, a long term destructive effect would be expected. In this project, further experimental investigations are planned to be able to prove the link between the aerodynamic effects and main shaft motion. Simulation methods will also be used for comparison and validation.

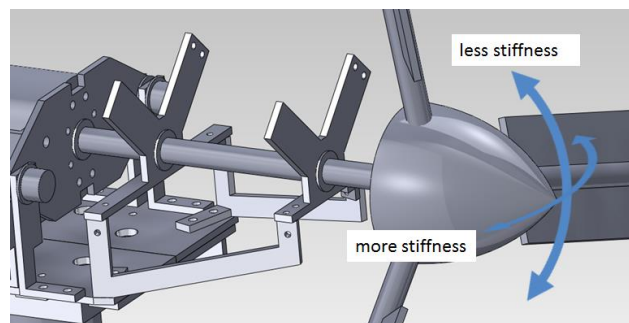


Figure 12. Main shaft framework stiffnesses

Another investigation can be performed with the experimentally obtained data when considering the theory of fatigue in regards to repetitive loading of components or system members. As described earlier, the horizontal movements are rather small compared to the vertical

oscillations so that for a simplified approach only the vertical displacements are considered. It is obvious that the peaks of the displacements group in different ranges with different numbers of reoccurrences and a statistical approach can be taken. Since the two bearings move somewhat synchronously only the data for Bearing 1 is considered here. A data peak histogram was created using

data similar to that shown in Figure 11, from a time record covering 20 seconds. The number of peaks in the range between 0 mm and 0.0025 mm was 2373, the number of peaks in the range between 0.0025 mm and 0.0075 mm was 2480, the number of peaks in the range between 0.0075 mm and 0.0125 mm was 264, and between 0.0125 mm and 0.0175 mm was 6.

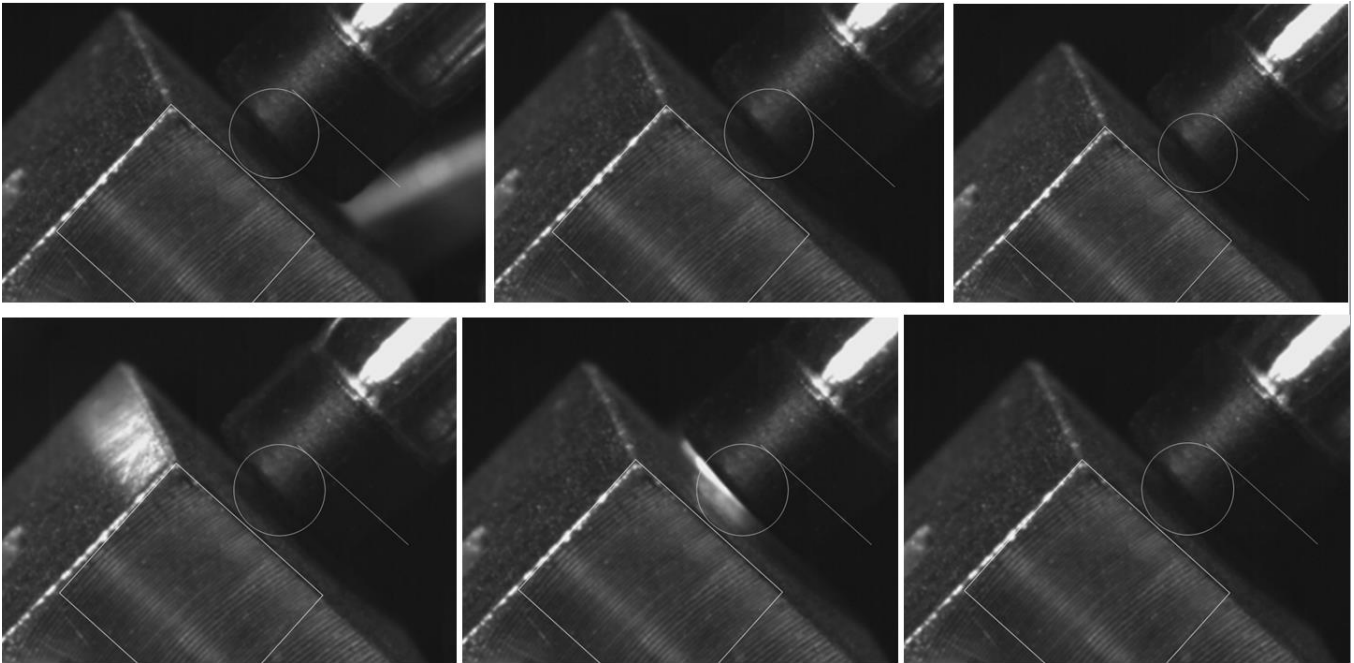


Figure 13. High speed camera sequence of proximity probe tip

Over the given timeframe of the experiment, with a simple extrapolation, it could be calculated that these numbers reach  $10^6$  cycles after 8428s or 2.34h for the 0 mm to 0.0025 mm range, 8064s or 2.3h for the 0.0025 mm to 0.0075 mm range, 75757s or 21h for the 0.0075 mm to 0.0125 mm range and 3333333s or 39 days for the 0.0175 mm to 0.0125 mm range.

The  $10^6$  cycle number has a special meaning in fatigue theory, being the critical number of cycles for members made of steel at which failure and component lifetime can be measured. In a so called S-N curve, a member loaded repeatedly above the limit specified in the S-N curve will fail before reaching  $10^6$  cycles, whereas the member loaded below this critical limit, will survive, theoretically forever. Given the typical lifetime until failure of five years for wind turbine gearboxes, it could be hypothesized that the simple approach of this repetitive bending theory for this application in this experiment from a fatigue point of view would not primarily contribute to a failure of a gearbox part. Further research is however planned to be conducted to investigate, if such behaviour of the main shaft also exists in larger scale wind turbines with similar main shaft and

bearing design, and if the motion pattern, displacements and cycle numbers are similar.

To optically obtain an impression of the movement of the bearings, and hence the main shaft as well as the hub of the rotor, footage has been recorded with a high speed camera.

Figure 13 shows a sequence of pictures of the motion of one front bearing block from its maximum point of distance to its minimum point of distance to the front tip of a proximity probe. The single line, visible in the picture is fixed onto a distinctive dot on the probe front. The circle has been inserted as an object being fixed at the single line and reaching close to the surface of the block that is connected with the moving bearing holder. The radius of the circle is constant throughout the sequence. The square has been aligned with features of the block and is shifting with the movement relative to the circle. Since the displacements are rather small, it is hard, if not impossible to make out any change in the distance between the circle and the square, here in this picture, but if the sequence is switched through in rapid succession on a computer screen, the movement is obvious.

## 5. CONCLUSION

An introduction has been given into research investigating the cause for premature wind turbine gearbox failures. At the current stage an experimental wind turbine test rig set up exists in a laboratory. The wind flow environment, created by a fan has been quantified by measurements and roughly defined. Turbulences in the flow, which are assumed to be the cause for the gearbox damage have been considered by assuming unequal aerodynamic forces on rotor blades, which create a resulting fluctuating moment at the rotor hub. It is intended to artificially increase the intensity of turbulences by objects being placed in the wind flow and record and analyse the effect on the test rig.

Until now, measurements have been conducted with proximity probes to measure the displacement of the main shaft at bearing positions due to the resulting moment at the hub. It has been found that a dominant repetitive bending movement in the vertical plane exists. Two hypotheses have been stated as to what effect this bending could have on the first bearing of the gearbox and the gearbox wall. In both cases, the effect of the motion of the main shaft is suspected to have a long term damaging effect inside the gearbox. In further investigations it is planned to simulate a gearbox with suitable software and use the real life data, obtained in these experiments, as simulated input motion at the gearbox entrance. Also experimental measurements of displacements, bending angles and stresses at the interface between the main shaft and gearbox wall on the test rig are anticipated.

A further investigation has revealed by using simple fatigue theory, that the repetitive bending for certain ranges of displacements reaches critical numbers long before the gearbox lifetime of five years. This does not exclude that this motion is not contributing to the failure but a direct link to a critical number close to five years has not been established.

In the experiment a high speed camera was used to optically capture the motion of the main shaft. This device is intended to be used further in the project to verify test data as far as it is possible and to investigate and make visible any displacements that occur. In particular when the intensity of the turbulent flow is increased it is hoped to see more obvious effects on the components.

As this paper is only focusing on the main shaft movement which was the first goal of this research, there are more additions of sensors planned in the experimental set up. For example, strain gauges have already been installed on all three blade roots and two encoder wheels with optical switches have been installed on the main shaft which provide further concurrent experimental data to give a broader picture of the effects that take place during operation. It is also intended to install more sophisticated

blades as compared to the crude ones which are currently fitted to the hub.

As for the wind environment, it is planned to obtain a more precise picture of the flow pattern downstream of the wind source and straightener device as well as a more sophisticated means of quantifying turbulent flow. Where suitable, flow simulation software will be used to aid in confirming the experimental values gathered.

Multiple variations of factors such as mentioned above are planned with the aim to better understand causes of wind turbine gearbox failures. At the moment the project looks at the aspects of aerodynamics, vibration and gear and bearing wear from a more distant vintage point and rather investigates how these three areas have a combined effect onto the system. Where deemed suitable, a closer look into certain components and under certain operating conditions will be performed in future experiments and subprojects.

## REFERENCES

- Musial, W., and Butterfield, S., McNiff, B. (2007). *Improving Wind Turbine Gearbox Reliability Analysis of Electronic Prognostics*. European Wind Energy Conference Milan, Italy, May 7-10, 2007. <http://www.citeseerx.ist.psu.edu/viewdoc/download?doi=10.1.1.114.8227&rep=rep1&type=pdf> (accessed June 28, 2010)
- Heller, A., (2010), Science & Technology Review *Extracting More Power from the Wind*. April/May 2010. <https://str.llnl.gov/AprMay10/tmirocha.html> (accessed October 6, 2010)
- Van Rensselaar, J. (2010), Tribology & Lubrication Technology. *The Elephant*. [http://www.stle.org/assets/news/document/Cover\\_Story\\_06-10.pdf](http://www.stle.org/assets/news/document/Cover_Story_06-10.pdf) (accessed October, 2010)
- Moser, B., (2010). *Turbine Failure: Fine-tuning turbine gearbox performance*. <http://social.windenergyupdate.com/industry-insight/turbine-failure-fine-tuning-turbine-gearbox-performance> (accessed October 7, 2010)
- Pope, A., Harper, J. J. (1966). *Low-Speed Wind Tunnel Testing*. NJ: John Wiley & Sons, Inc
- Rexroth Bosch Group (2010). *Innovative Gearboxes for Wind Turbines*. [http://www.mywindpowersystem.com/marketplace/wp-content/uploads/2010/04/Bosch-Rexroth-2\\_5mW-Gearbox-Technical-Information-pdf.pdf](http://www.mywindpowersystem.com/marketplace/wp-content/uploads/2010/04/Bosch-Rexroth-2_5mW-Gearbox-Technical-Information-pdf.pdf) (accessed December 12, 2010)
- Juvinall, R. C., Marshek, K. M. (2006). *Fundamentals of MACHINE COMPONENT DESIGN*. John Wiley & Sons, Inc
- Eck, B. (1973). *Fans*. Oxford, Pergamon Press Ltd.